Excitonic properties of $Zn_{1-x}Cd_xSe/ZnSe$ strained quantum wells

V. Pellegrini, R. Atanasov, A. Tredicucci, and F. Beltram
Scuola Normale Superiore, I-56126 Pisa, Italy

C. Amzulini, L. Sorba,* L. Vanzetti, and A. Franciosi†
Laboratorio Tecnologie Avanzate Superfici e Catalisi dell' Istituto Nazionale di Fisica della Materia, I-34012 Trieste, Italy

(Received 8 July 1994; revised manuscript received 23 September 1994)

We present a systematic investigation of the linear optical properties of $Zn_{1-x}Cd_xSe/ZnSe$ multiple quantum well structures in the excitonic region using absorption and photoluminescence measurements in the 10–300 K temperature range. Heavy- and light-hole excitonic transitions and heavy-hole exciton binding energies were measured for different well widths and compositions. A set of consistent parameters was determined within a two-band model, which accurately describes the excitonic properties of the strained $Zn_{1-x}Cd_xSe$ quantum wells.

An intense research effort is currently being devoted to clarifying the optical properties of wide-gap II-VI semiconductor heterostructures. This interest stems primarily from the possibility of obtaining laser diodes and other optoelectronic and photonic devices operating in the blue region of the visible spectrum.[1,2] Blue-green lasers exploiting $Zn_{1-x}Cd_xSe/ZnSe$ multiple quantum wells (QW's) as active materials have been recently demonstrated and the strong nonlinear excitonic properties of these materials represent a further new and exciting subject of investigation. However, such studies require a preliminary thorough understanding of the linear excitonic properties together with the evaluation of several important band parameters such as the fraction of the band-gap difference which appears in the valence band (Q_v) and the in-plane effective masses. Band offsets in particular play a central role in determining electron and hole confinement energies and therefore strongly influence the excitonic optical properties. For $Zn_{1-x}Cd_xSe/ZnSe$ QW's, to the best of our knowledge, no direct measurement of the band offset is available, although several authors have assumed or calculated values of Q_v in the 0.17–0.36 range.[3–6]

Recent efforts to model optical spectral features have achieved some success by using a combination of four-band and two-band models applied to the calculation of the measured optical absorption spectra for three QW samples with nominal $x = 0.25$, at a temperature of 10 K.[3] We have studied a larger set of samples carrying out systematic absorption and photoluminescence (PL) measurements that yielded excitonic transitions and binding energies in $Zn_{1-x}Cd_xSe/ZnSe$ QW's as a function of temperature, alloy composition and well width. Exploiting a model recently developed,[7,8] we derived, from the experimental data, a set of consistent parameters (including Q_v) that accurately reproduce the measured exciton binding energies and the heavy- and light-hole $1s$ excitonic transitions.

All samples were grown by solid source molecular-beam epitaxy on GaAs(001) substrates and consisted of a 0.5-μm GaAs buffer layer grown at 580 °C, a 1.5-μm ZnSe buffer layer grown at 290 °C, ten $Zn_{1-x}Cd_xSe/ZnSe$ QW's grown at 250°C with a 30-s growth interruption at each interface, and a 500-nm-thick ZnSe cap layer grown at the same temperature. More details on the growth procedure, the background doping of the nominally undoped layers, and the x-ray diffraction calibration of layer composition and width can be found elsewhere.[2,9,10] $Zn_{1-x}Cd_xSe$ well widths in the 2–5 nm range were examined for two different Cd concentrations ($x = 0.1$ and $x = 0.31$). The ZnSe barrier width was 30 nm in all cases.

All samples were characterized between 10 K and room temperature. PL measurements were performed using the 458-nm line of an Ar-ion laser focused at 45° from the [001] growth direction z, with an incident intensity of about 1 W/cm^2. The PL emission was collected in backscattering geometry along the z direction and dispersed by a 0.004-nm-resolution monochromator. For absorption measurements, the samples were mechanically thinned down to about 50 μm and circular areas of the GaAs substrate about 6×10^{-4} cm^2 in size were selectively removed using standard photolithographic and wet-etching techniques. PL spectra recorded before and after substrate removal showed no change, ruling out mechanical damage to the structures. Transmission measurements were performed using a 100-W xenon lamp as the source.

Absorption spectra at 10 K for $Zn_{1-x}Cd_xSe/ZnSe$ QW's (Ref. 11) with $x = 0.31$ and $x = 0.10$ are shown in Figs. 1(a) and 1(b), respectively. For comparison, we also show in Fig. 1(a) the PL spectrum of a $x = 0.31$, 5-nm-thick QW structure recorded at the same temperature (dashed line). The corresponding measured Stokes shift was about 1 meV. Analogous Stokes shifts were measured for the 4-nm-wide QW's, but larger shifts (10 meV) were observed in the 2- and 3-nm-thick wells.[12]

In all absorption spectra in Fig. 1 at least two peaks are observed. Three absorption peaks are instead found in the spectrum of the two wider wells with $x = 0.31$. In

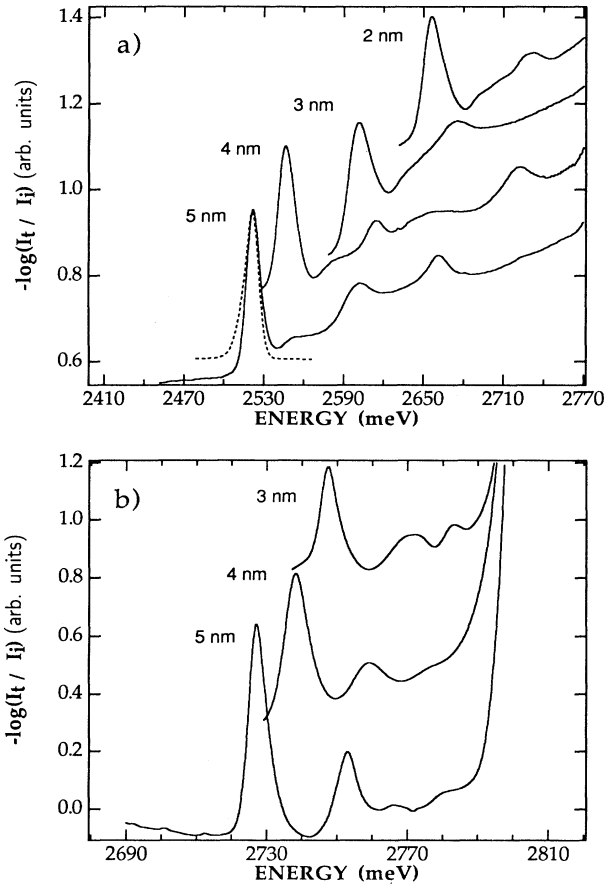

FIG. 1. Absorption spectra of $Zn_{1-x}Cd_xSe/ZnSe$ samples at 10 K with (a) $x = 0.31$ and (b) $x = 0.1$. Each spectrum is labeled by the well width. For comparison we also show in (a) a representative PL spectrum at 10 K (dotted line) from one of the samples.

order to identify the corresponding transitions, we have analyzed the polarization dependence of the absorption in selected samples. To this end, we recorded absorption spectra using linearly polarized light incident at an angle of about 60° relative to z, for different polarization directions. Since, contrary to light-hole (lh) -related excitonic transition, heavy-hole (hh) transitions are allowed only for polarization in the QW plane, by varying the in-plane component of the electric field, the origin of the different transitions can be established. For example, in the sample with a 5-nm-thick QW and $x = 0.31$, with increasing in-plane component of the electric field we observed an increase in the intensity of the first and third spectral features, while the second one remained largely unchanged. This proves the hh character of the two lateral absorption peaks. The second absorption feature is therefore unambiguously identified as an $n = 1$ lh exciton.

The low-temperature full width at half maximum (FWHM) of the lowest energy absorption feature, ascribed to the $n = 1$ hh excitonic transition, ranges between 5 meV ($x = 0.1$) and 10 meV ($x = 0.31$) in the 10-QW samples examined, while single QW's with $x = 0.31$ exhibited FWHM's of only a few meV.[13] Such reduced linewidths compare very favorably with recent results on the same material system.[1] We also note that the onset of the hh continuum is clearly detected in the absorption spectra for the $x = 0.31$ QW's in Fig. 1(a). Table I summarizes the main features observed in our samples, i.e., energies of photoluminescence and absorption exciton peaks and measured continuum edges.

The temperature dependence of the spectra was studied up to room temperature (RT). At RT, the lh-exciton absorption is weakly identifiable only in the spectra from the wider QW's with $x = 0.31$. In all other cases, no lh signal was detected throughout the 200–300 K temperature range. The temperature dependence of the width and position of the hh-exciton line is quite similar to that observed in III-V QW's, and from the usual fitting procedure of the spectral line shape we have found a value $\Gamma_{LO} = 33.2$ meV for the Fröhlich coupling constant, comparable to those reported in the literature.[6]

We modeled the excitonic optical properties within a variational two-band framework which accounts for the effective-mass mismatch and anisotropy, as well as for the dielectric mismatch.[7] This model was recently successfully applied to strained III-V QW's.[8] The starting point of the calculation is the determination of the cadmium-concentration dependent electron $[m_e(x)]$ and hole $[m_\beta(x),\beta = \text{hh,lh}]$ effective masses along the z direction. These were estimated through a linear interpolation of ZnSe-related and zinc-blende CdSe-related bulk values (see Table II). The corresponding in-plane hole masses

TABLE I. Position of the main spectral features observed in multiple quantum well samples at 10 K, as a function of the quantum well width (L_w) and the nominal Cd concentration (x). The values reported correspond to the observed energies (in meV) of heavy- (hh1-e1) and light-hole (lh1-e1) exciton peaks as obtained by photoluminescence (PL) and absorption (abs) measurements and to the energy of the hh1-e1 continuum onset edges (cont) measured in the absorption spectra of the $x = 0.31$ QW's as described in the text.

L_w (nm)	Cd	hh1-e1 PL	hh1-e1 abs.	hh1-e1 cont.	lh1-e1 abs.
3	$x = 0.1$		2747.3		2771
4	$x = 0.1$		2738.1		2759.6
5	$x = 0.1$		2727.1		2753.3
2	$x = 0.31$	2648.5	2656.4	2689.4	2729.6
3	$x = 0.31$	2588.5	2601.3	2634.3	2673.6
4	$x = 0.31$	2541.5	2546.4	2577.4	2614.1
5	$x = 0.31$	2520.5	2522	2547	2600.5

TABLE II. Physical parameters of ZnSe and cubic CdSe bulk materials. Parameters given in bold represent, together with Q_v, our fitting parameters. All the remaining values, with the exception of the ZnSe heavy-hole mass m_{hh} (Ref. 18) and the CdSe stiffness constants C_{11} and C_{12} (Ref. 19) are taken from Ref. 20.

	ZnSe	CdSe
a_0 (Å)	5.6676	6.052
C_{11} (N/m^2)	$8.59\pm0.3 \times 10^{10}$	6.67×10^{10}
C_{12} (N/m^2)	$5.06\pm0.2 \times 10^{10}$	4.63×10^{10}
a (eV)	−5.4	**−3.45**
b (eV)	−1.2	**−0.8**
m_e	0.14	0.11
m_{hh}	0.49	0.45
m_{lh}	0.145	**0.145**
ε_B	8.7	**8.7**
E_g (eV) at 0 K	2.82	1.9

can then be expressed in terms of $m_\beta(x)$,[14]

$$m_{hh||}(x) = 4[1/m_{hhz}(x) + 3/m_{lhz}(x)]^{-1},$$
$$m_{lh||}(x) = 4[1/m_{lhz}(x) + 3/m_{hhz}(x)]^{-1}. \quad (1)$$

The electron mass was assumed to be spherically symmetric.

Confinement potentials for electrons and holes were calculated as a function of $Q_v = V_{hh}/\Delta E_{gS}$. Here V_{hh} is the hh-band discontinuity, and $\Delta E_{gS} = V_e + V_{hh}$ is the band-gap difference, including the built-in strain. In our $Zn_{1-x}Cd_xSe$/ZnSe compressively strained QW's, the band gap in the barrier coincides with the band gap of bulk ZnSe. Inside the well, it is determined as the energy separation between the bottom of the conduction band and the top of the hh band (E_{gS}^{hh}). Similarly, the lh band is separated from the conduction-band by an energy gap E_{gS}^{lh} ($E_{gS}^{lh} > E_{gS}^{hh}$). These quantities can be calculated taking into account the unstrained $Zn_{1-x}Cd_xSe$ band gap $E_g(x)$ and the hydrostatic and uniaxial compressive strain energies δE_H and δE_S:

$$E_{gS}^{hh} = E_g(x) + \delta E_H - \delta E_S,$$
$$E_{gS}^{lh} = E_{gS}^{hh} + 2\delta E_S + \frac{1}{2}\left[\Delta_0 - \delta E_S - \sqrt{(\Delta_0 - \delta E_S)^2 + 8\delta E_S^2}\right], \quad (2)$$

where Δ_0 is the unstrained split-off energy. $E_g(x)$ is given by[15]

$$E_g(x) = E_g^{ZnSe} + (E_g^{CdSe} - E_g^{ZnSe} - B)x + Bx^2, \quad (3)$$

where $B = 350$ meV. Finally, the x-dependent strain energies δE_H and δE_S are expressed by the relative cell deformation δ_L [$\delta_L = a_0(0)/a_0(x) - 1$] as follows:

$$\delta E_H(x) = 2a(x)(1 - C_{12}/C_{11})\,\delta_L,$$
$$\delta E_S(x) = b(x)(1 + 2C_{12}/C_{11})\,\delta_L, \quad (4)$$

where $a_0(x)$ is the lattice parameter of the alloy, $C_{11}(x)$ and $C_{12}(x)$ are the alloy stiffness constants, and $a(x)$ and $b(x)$ denote the deformation potentials. Equations (2) and (4) together with the choice of Q_v uniquely determine the electron- and hole-confinement potentials. All the strain parameters appearing in these equations were obtained by linear interpolation of the bulk values given in Table II.

Making use of the effective masses and QW potential profiles described above, we calculated the hh-exciton states by a variational procedure.[7] The variational solution is sought by minimizing the exciton energy $E_{ij}^\beta[\lambda_{ij}^\beta]$ as a function of the two-dimensional (2D) exciton radius (λ_{ij}^β); here i (j) labels the electron (hole) subband. The continuum transition energy is mostly affected by Q_v and the deformation potentials, while the background dielectric function $\varepsilon_B(x)$ of $Zn_{1-x}Cd_xSe$ influences the exciton binding energy (R_{ij}). We show in Figs. 2(a) and 2(b) our results for the calculated $1S$ excitonic transition energies E_{11}^{hh} as a function of the QW width (L_w) for the two different Cd concentrations (thick dotted lines). The experimental values of the transition energies, as measured from the absorption (PL) spectra are denoted by solid (open) triangles. Horizontal error bars denote

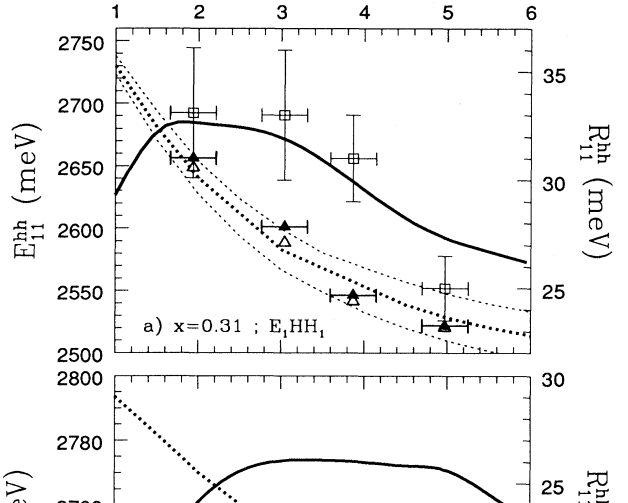

FIG. 2. Calculated $1S$ heavy-hole exciton binding energies (solid line, right vertical scale) and heavy-hole hh1-e1 exciton transition energies (dotted lines, left vertical scale) plotted as a function of the well width L_w for Cd concentrations (a) $x = 0.31$ and (b) $x = 0.1$. In (a) the upper and lower dotted curves have been calculated for $x = 0.33$ and $x = 0.29$, respectively. Experimental results for absorption (▲), photoluminescence (△), and exciton binding energies (□) are also shown.

an estimated uncertainty of one monolayer in the QW widths; vertical error bars correspond to the experimental broadening of the continuum absorption edge. For both samples, best agreement between theory and experiment was obtained with $Q_v = 0.25$, $a^{\mathrm{CdSe}} = -3.45$, and $b^{\mathrm{CdSe}} = -0.8$. The thin dotted lines in Fig. 2(a) refer to calculated values of E_{11}^{hh} with a 0.02 variation in x. The strong dependence of the transition energy on this parameter is clearly observed. In Fig. 2 we also show the calculated value of R_{ij} (solid curve, right vertical scale) and the corresponding experimental values for the $x = 0.31$ alloy (open squares). The results indicate that the well width yielding maximum exciton confinement would be in the 3-nm range for $x = 0.31$ and in the 4.5-nm range for $x = 0.1$. The calculation was performed with the same value for ε_B in ZnSe and CdSe, since upon introducing a reasonable dielectric mismatch we did not observe significant improvements in the agreement between theory and experiment. We mention that the estimated value of $\varepsilon_{\mathrm{CdSe}}$ should be regarded as a model-dependent value, including possible polaronic effects.[16,17] Such effects could be taken into account by making use of the polaronic Hamiltonian (see, for example, Refs. 16 and 17). This procedure would require a set of new material parameters characterizing the electron-phonon interaction. To our knowledge these parameters are not yet available for zinc-blende CdSe crystals.

In general, the model reproduces remarkably well the data in Fig. 2. The only substantial discrepancy in Fig. 2(a) is observed for the hh-exciton binding energy in the sample with 5-nm-thick, $x = 0.31$ QW's, i.e., when L_w becomes larger than the exciton Bohr radius $\lambda_{11}^{\mathrm{hh}}$, violating the assumption of a purely 2D exciton. In this case the correlation between the e-h relative motion in the z direction with that in the in-plane directions cannot be neglected and a more complicated variational approach would be necessary.[8] The most interesting range, however, is that around the maximum binding energies;[1] in this region our 2D model yields accurate results.

Using the best-fit values for Q_v and the deformation potentials for the x values we studied, light holes experience a repulsive potential of several meV in the $Zn_{1-x}Cd_xSe$ region. The strong electron-hole Coulomb interaction becomes therefore the dominant factor in confining light-hole excitons in the well. We modeled this situation along the lines developed for strained $GaAs/Ga_{1-x}In_xAs$ QW's,[8] using the CdSe lh effective mass in the z direction as the fitting parameter. We introduce a box of length l_b, where the light hole states are fully confined [this is equivalent to add no-escape boundary conditions for the light-hole envelope functions u_j^{lh}, i.e., $u_j^{\mathrm{lh}}(\pm l_b/2) = 0$]. The appropriate value for l_b depends on Coulomb electron-hole interaction, as well as on band mismatch in the well region. To take into account both factors, we consider l_b as a variational parameter and perform a minimization of the total exciton energy $E_{11}^{\mathrm{lh}}[l_b, \lambda_{11}^{\mathrm{lh}}]$ with respect to the box length and the exciton radius $\lambda_{11}^{\mathrm{lh}}$. We show in Figs. 3(a) and 3(b) our results for the calculated $1S$ excitonic transition energies E_{11}^{lh} as a function of the QW width (L_w) for the two different Cd concentrations (dotted lines). The experimental values are denoted by solid triangles. We emphasize that the calculated lh-exciton energies are very sensitive to the choice of Q_v and x, so that the good agreement between theory and experiment in Fig. 3 strongly supports the values of the parameters derived in this work.

An independent test of our model was performed using the same parameter set to calculate E_{11}^{hh} and E_{11}^{lh} in the $Zn_{1-x}Cd_xSe/ZnSe$ QW's of Ref. 3. Using the nominal Cd concentration ($x = 0.25$) and nominal well widths of Ref. 3, we reproduced very accurately the experimental transition energies (well within a one-monolayer thickness fluctuation for the 3- and 6-nm wells). For the sample with $L_w = 9$ nm, we obtain a larger shift in the calculated lh and hh excitonic transitions. As we mentioned above, this can probably be linked to a deviation from the 2D behavior, as observed in the numerical simulation of our data.

In conclusion, we have presented a systematic experimental and numerical analysis of the exciton properties in a set of ZnCdSe/ZnSe QW's samples of different well widths and cadmium concentrations. With the combination of polarization-dependent absorption measurements and a two-band model for numerical analysis we have identified the heavy-light nature of the observed excitons. Coulomb interaction between electrons and light-holes has been found to be the dominant factor in confining light-hole excitons in the well and has been taken into ac-

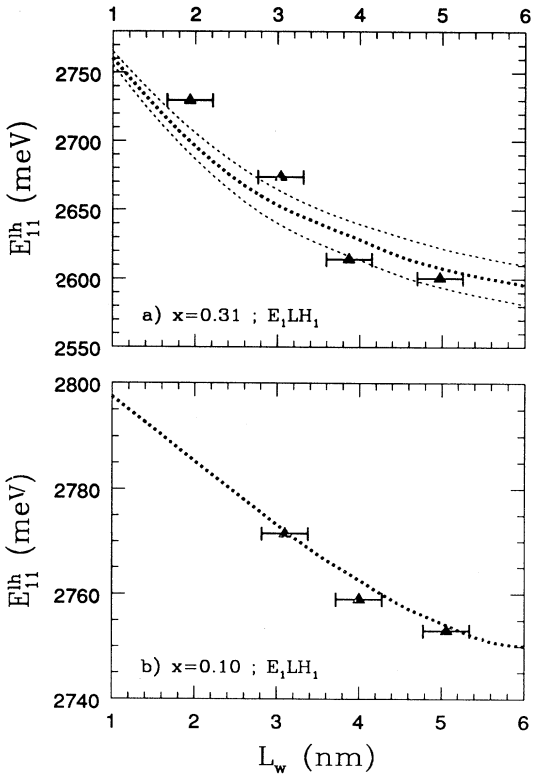

FIG. 3. Calculated $1S$ light-hole excitonic transition energy (dotted line) as a function of the well width L_w for the same samples examined in Fig. 2. In (a) the upper and lower dotted curves were calculated for $x = 0.33$ and $x = 0.29$, respectively. Experimental light-hole exciton transition energies (▲) are also shown.

count to reproduce the experimental results on light-hole (lh1-e1) exciton transitions. Using the exploited two-band model to fit the transition energy of heavy (hh1-e1) and light (lh1-e1) excitons and the hh1-e1 exciton binding energies we have obtained a set of consistent parameters.

This work was supported in part by the U.S. Army Research Office under Grant No. DAAH04-93-G-0206. We thank P. Sciacovelli and L. Tapfer (CNRSM, Brindisi, Italy) for the x-ray diffraction characterization of the samples and F. Bassani and R. Cingolani for useful discussions.

* Also at Istituto ICMAT del CNR, Montelibretti, Roma, Italy.

† Also at Department of Chemical Engineering and Materials Science, University of Minnesota, Minneapolis, Minnesota 55455.

[1] Y. Yamada, Y. Masumoto, J.T. Mullins, and T. Taguchi, Appl. Phys. Lett. **61**, 2190 (1992); J. Ding, H. Jeon, T. Ishihara, M. Hagerott, A.V. Nurmikko, H. Luo, N. Samarth, and J. Furdyna, Phys. Rev. Lett. **69**, 1707 (1992); J. Ding, M. Hagerott, T. Ishiara, H. Jeon, and A.V. Nurmikko, Phys. Rev. B **47**, 10 528 (1993).

[2] R. Cingolani, R. Rinaldi, L. Calcagnile, P. Prete, P. Sciacovelli, L. Tapfer, L. Vanzetti, G. Mula, F. Bassani, L. Sorba, and A. Franciosi, Phys. Rev. B **49**, 16 769 (1994); R. Cingolani, M. Di Dio, M. Lomascolo, R. Rinaldi, P. Prete, L. Vasanelli, L. Vanzetti, F. Bassani, A. Bonanni, L. Sorba, and A. Franciosi, *ibid.* **50**, 12 179 (1994).

[3] P.M. Young, E. Runge, M. Ziegler, and H. Ehrenreich, Phys. Rev. B **49**, 7424 (1994).

[4] Y. Kawakami, I. Hauksson, H. Stewart, J. Simpson, I. Galbraith, K.A. Prior, and B.C. Cavenett, Phys. Rev. B **48**, 11 994 (1993).

[5] H.J. Lozykowsky and V.K. Shastri, J. Appl. Phys. **69**, 3235 (1991).

[6] J. Ding, N. Pelekanos, A.V. Nurmikko, H. Luo, N. Samarth, and J.K. Furdyna, Appl. Phys. Lett. **57**, 2885 (1990).

[7] R. Atanasov and F. Bassani, Solid State Commun. **84**, 71 (1992).

[8] R. Atanasov, F. Bassani, A. D'Andrea, and N. Tomassini, Phys. Rev. B **50**, 14 381 (1994).

[9] L. Sorba, G. Bratina, A. Antonini, A. Franciosi, L. Tapfer, A. Migliori, and P. Merli, Phys. Rev. B **46**, 6834 (1992).

[10] G. Bratina, R. Nicolini, L. Sorba, L. Vanzetti, G. Mula, X. Yu, and A. Franciosi, J. Cryst. Growth **127**, 387 (1993); R. Nicolini, L. Vanzetti, G. Mula, G. Bratina, L. Sorba, A. Franciosi, M. Peressi, S. Baroni, R. Resta, A. Baldereschi, J.E. Angelo, and W.W. Gerberich, Phys. Rev. Lett. **72**, 294 (1994).

[11] The sample temperature was monitored by means of a detector directly connected to the cold finger of the closed-cycle refrigerator. Temperature readings were verified using the known temperature dependence of the onset of the continuum edge in the ZnSe-related absorption spectra.

[12] Further work is in progress to study the origin of such relatively large Stokes shifts, and also in light of the result of M. Gurioli, A. Vinattieri, J. Martinez-Pastor, and M. Colocci, Phys. Rev. B **50**, 11 817 (1994).

[13] V. Pellegrini (unpublished).

[14] Considering the values of the hh and lh masses reported in Table II, we obtain $m_{\mathrm{hh}||}(0.31) = 0.176$, $m_{\mathrm{lh}||}(0.31) = 0.304$ and $m_{\mathrm{hh}||}(0.10) = 0.176$, $m_{\mathrm{lh}||}(0.10) = 0.306$.

[15] J.C. Jans, J. Petruzzello, J.M. Gaines, and D.J. Olego, SPIE Proc. **1985**, 260 (1993). We remark on the consistency of the parameters in Eq. (3) with the values of Table II.

[16] H. Haken, *Quantum Field Theory of Solids* (North-Holland, Amsterdam, 1976).

[17] C. Aldrich and K.K. Bajaj, Solid State Commun. **22**, 157 (1977).

[18] B. Sermage and G. Fishman, Phys. Rev. B **31**, 2379 (1985).

[19] R.M. Martin, Phys. Rev. B **6**, 4546 (1972).

[20] *Numerical Data and Functional Relationship in Science and Technology*, edited by O. Madelung, Landolt-Börnstein, New Series, Group III, Vol. 17, Pts. a and b (Springer, Berlin, 1982).